

CHAPTER 20

Materials Selection



The manufacturer of this carbon-fiber reinforced composite bicycle uses a sophisticated software package [utilizing “finite element analysis”] to analyze how the frame will respond to stress, allowing the engineers to tailor the frame stiffness to the individual rider. (Courtesy of Algor, Inc.)

Specifications

UNS number. A92036

Chemical Composition

Composition limits. 0.50 max Si; 0.50 max Fe; 2.2 max Cu; 0.10 to 0.40 Mn; 0.30 to 0.6 Mg; 0.10 max Cr; 0.25 max Zn; 0.15 max Ti; 0.05 max others (each); 0.15 max others (total); bal Al

Applications

Typical uses. Sheet for auto body panels

Mechanical Properties

Tensile properties. Typical, for 0.64 to 3.18 mm (0.025 to 0.125 in.) flat sheet, T4 temper; tensile strength, 340 MPa (49 ksi); yield strength, 195 MPa (28 ksi); elongation, 24% in 50 mm or 2 in. Minimum, for 0.64 to 3.18 mm flat sheet, T4 temper; tensile strength, 290 MPa (42 ksi); yield strength, 160 MPa (23 ksi); elongation, 20% in 50 mm or 2 in.

Hardness. Typical, T4 temper: 80 HR15T
strain-hardening exponent, 0.23

Elastic modulus. Tension, 70.3 GPa (10.2×10^6 ksi); compression, 71.7 GPa (10.4×10^6 ksi)

Fatigue strength. Typical, T4 temper: 124 MPa (18 ksi) at 10^7 cycles for flat sheet tested in reversed flexure

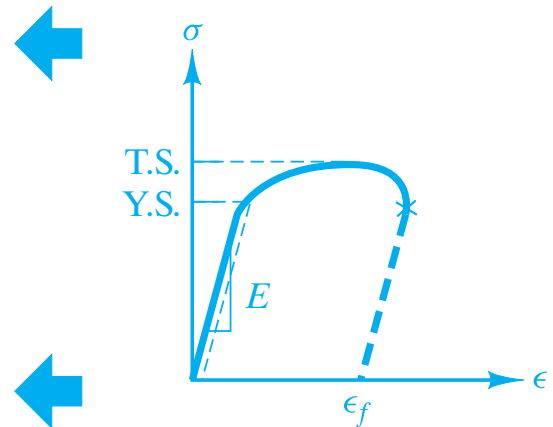


Figure 20-1 The basic mechanical properties obtained from the tensile test introduced in Chapter 6 lead to a list of engineering design parameters for a given alloy. (The parameters are reproduced from a list in ASM Handbook, Vol. 2, ASM International, Materials Park, Ohio, 1990.)

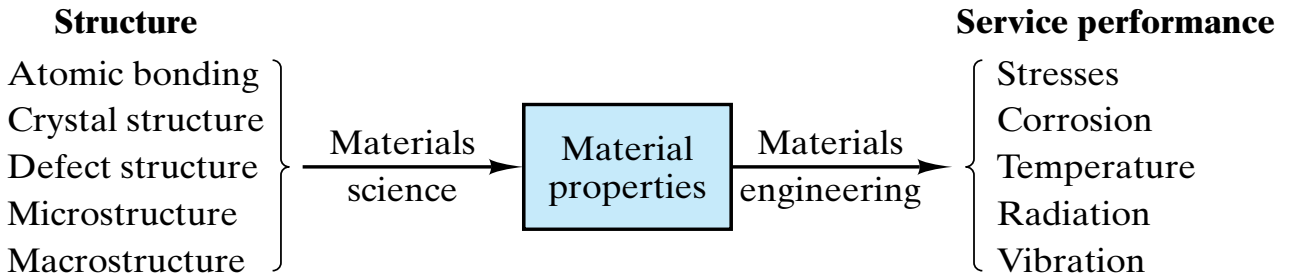


Figure 20-2 Schematic illustration of the central role played by properties in the selection of materials. Properties are a link between the fundamental issues of materials science and the practical challenges of materials engineering. (From G. E. Dieter, in *ASM Handbook, Vol. 20: Materials Selection and Design*, ASM International, Materials Park, Ohio, 1997, p. 245.)

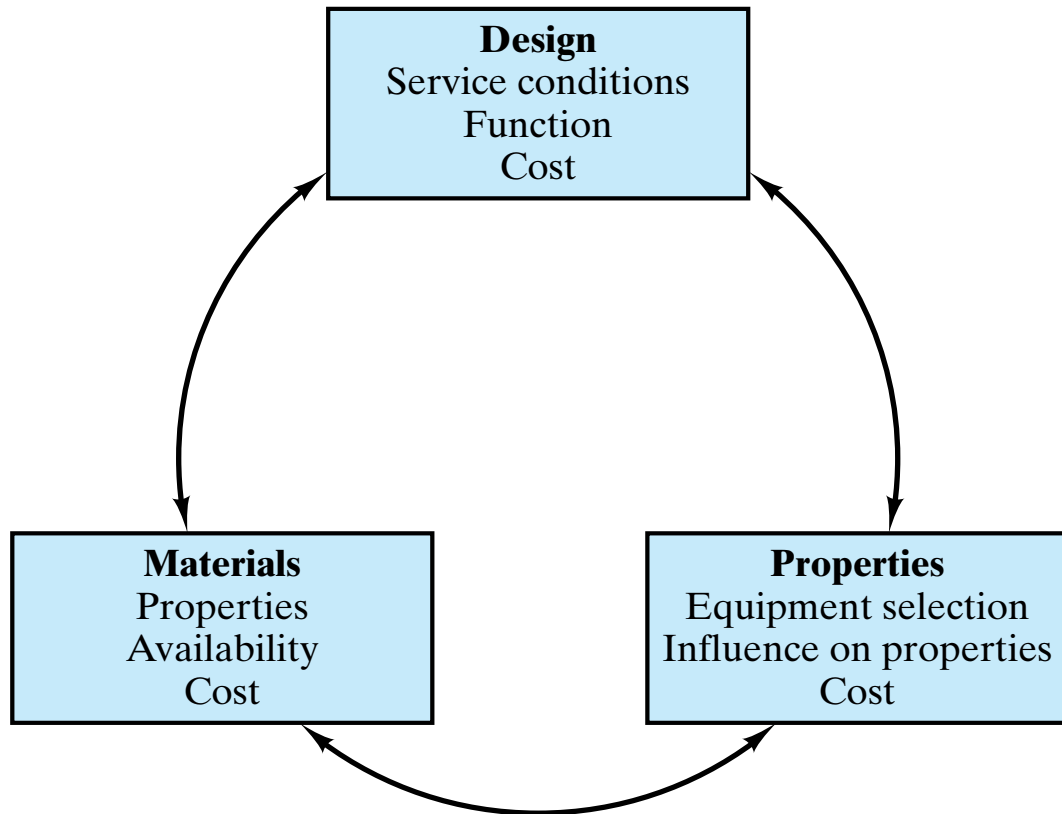


Figure 20-3 Schematic illustration of the integral relationship among materials, the processing of those materials, and engineering design. (From G. E. Dieter, in *ASM Handbook, Vol. 20: Materials Selection and Design*, ASM International, Materials Park, Ohio, 1997, p. 243.)

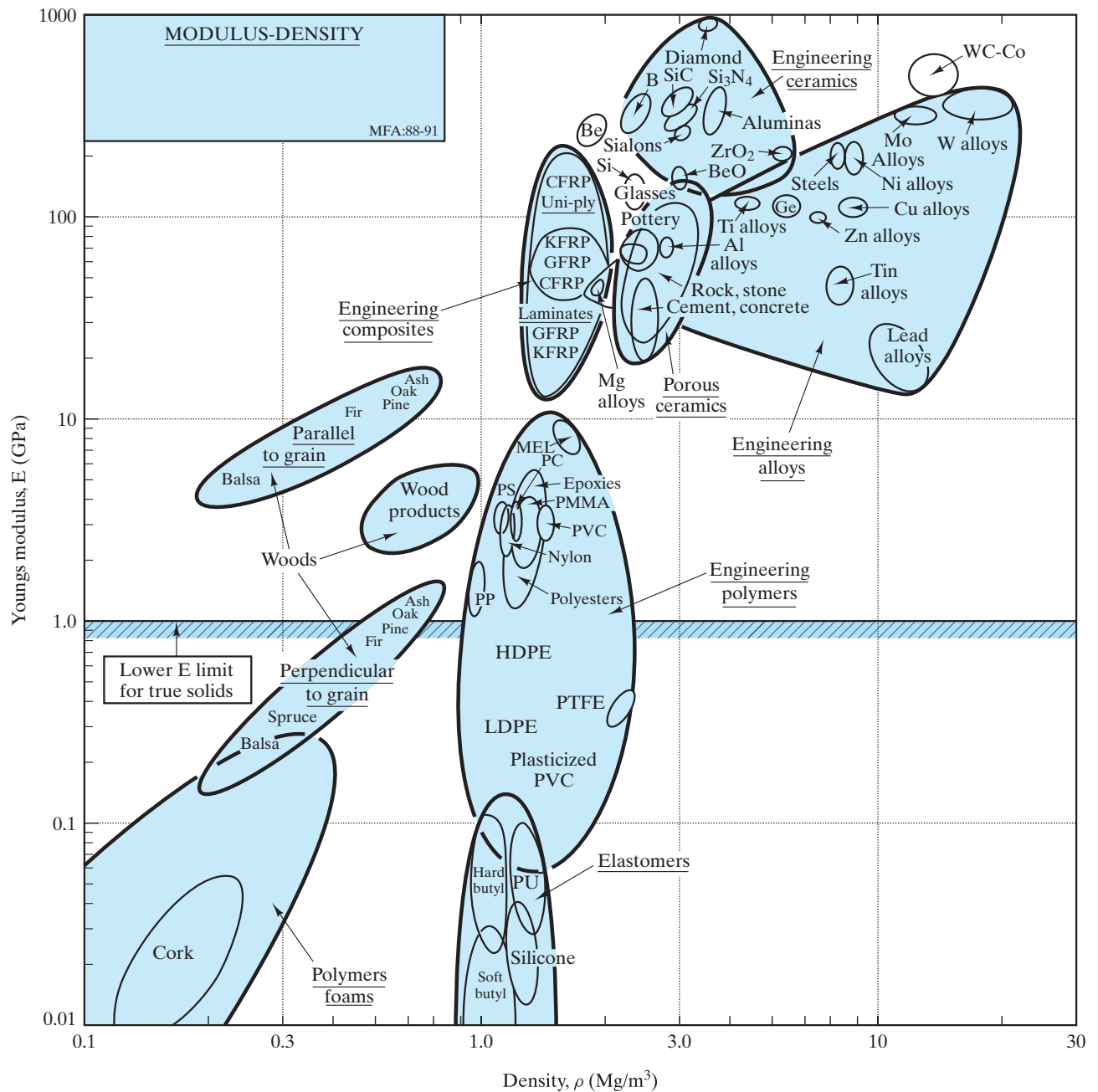


Figure 20-4 A materials property chart with a global view of relative materials performance. In this case, plots of elastic modulus and density data (on logarithmic scales) for various materials indicate that members of the different categories of structural materials tend to group together. (After M. F. Ashby, *Materials Selection in Engineering Design*, Pergamon Press, Inc., Elmsford, N.Y., 1992.)

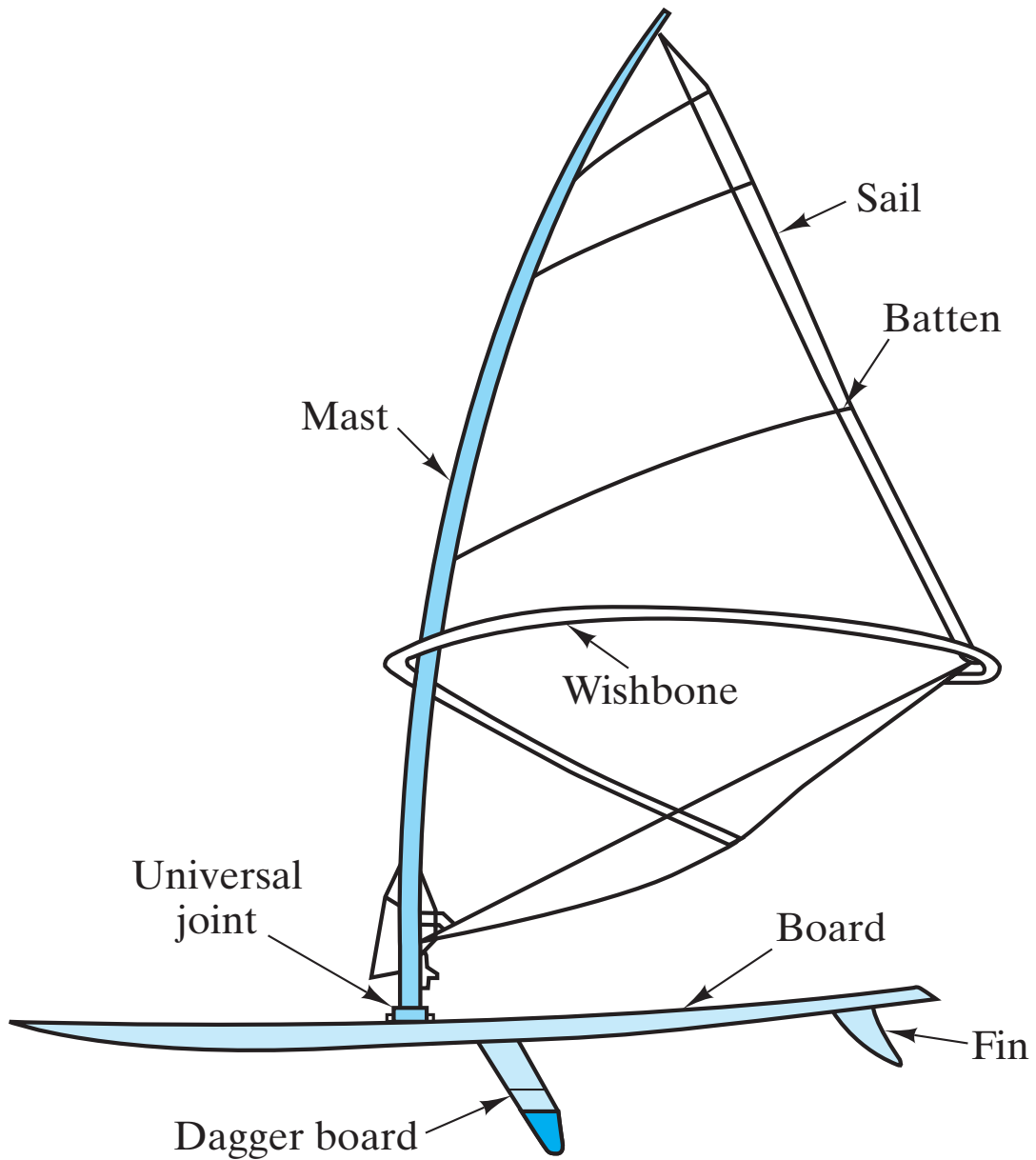


Figure 20-5 *Components of a windsurfer design. The stiffness of the mast controls the sail shape, and the pivoting of the mast about the universal joint controls the response of the craft. (After M. F. Ashby, "Performance Indices," in ASM Handbook, Vol. 20: Materials Selection and Design, ASM International, Materials Park, Ohio, 1997, pp. 281–290.)*

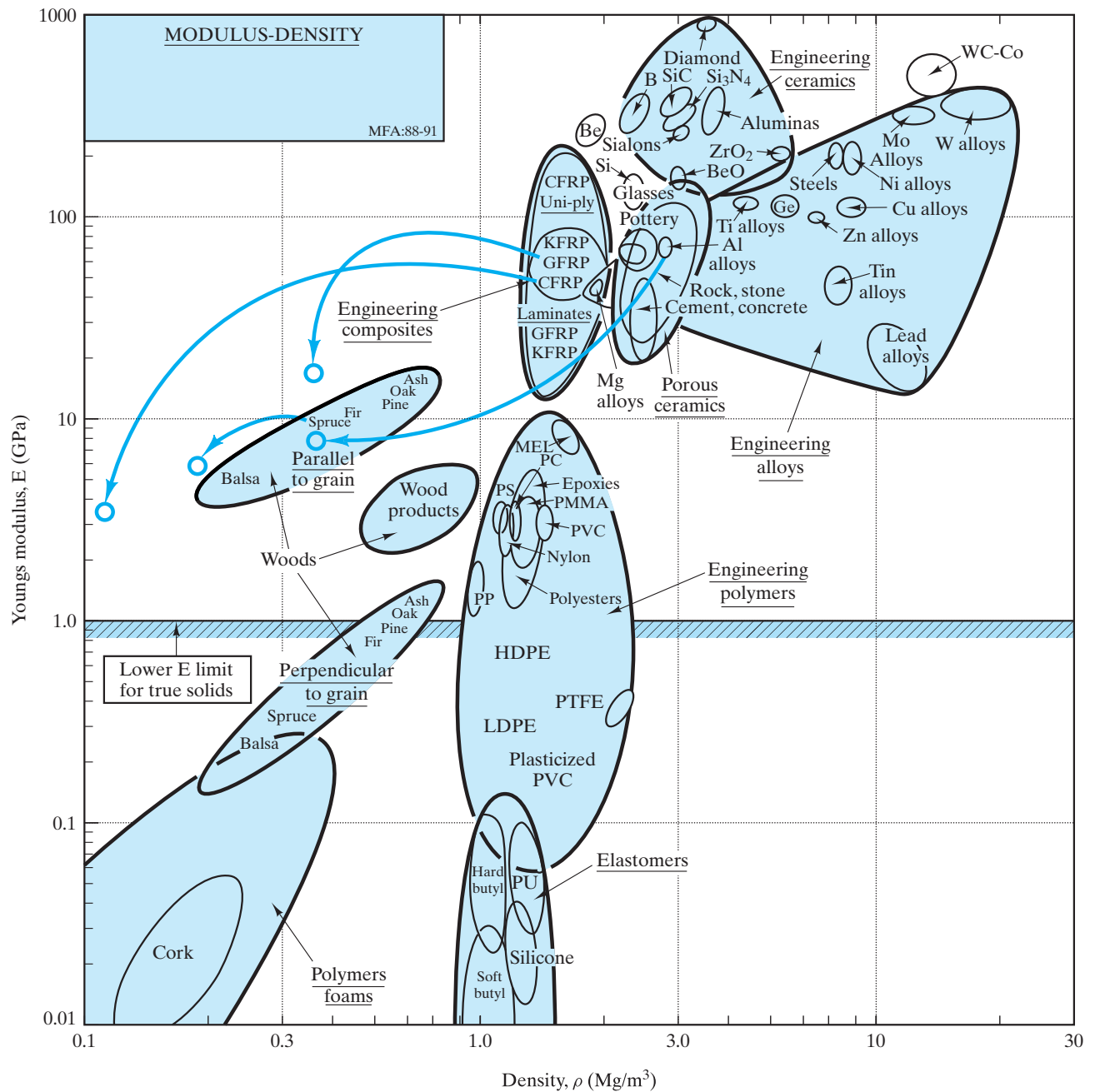


Figure 20-6 The behavior of the windsurfer mast materials in Table 20.4 are superimposed on the $\ln E$ versus $\ln \rho$ chart of Figure 20-4 normalized by the shape factor, ϕ , of a thin-walled tube. For example, the CFRP mast with a shape factor of $\phi = 14.3$ is shown at a position of $(E/14.3, \rho/14.3)$ relative to the (E, ρ) position of the bulk material for which $\phi = 1$. (After M. F. Ashby, "Performance Indices," in *ASM Handbook, Vol. 20: Materials Selection and Design*, ASM International, Materials Park, Ohio, 1997, pp. 281-290.)



Figure 20-7 *A drive sprocket made from dispersion-toughened nylon has replaced aluminum and steel parts in many motocross racing designs. (Courtesy of the Du Pont Company, Engineering Polymers Division)*

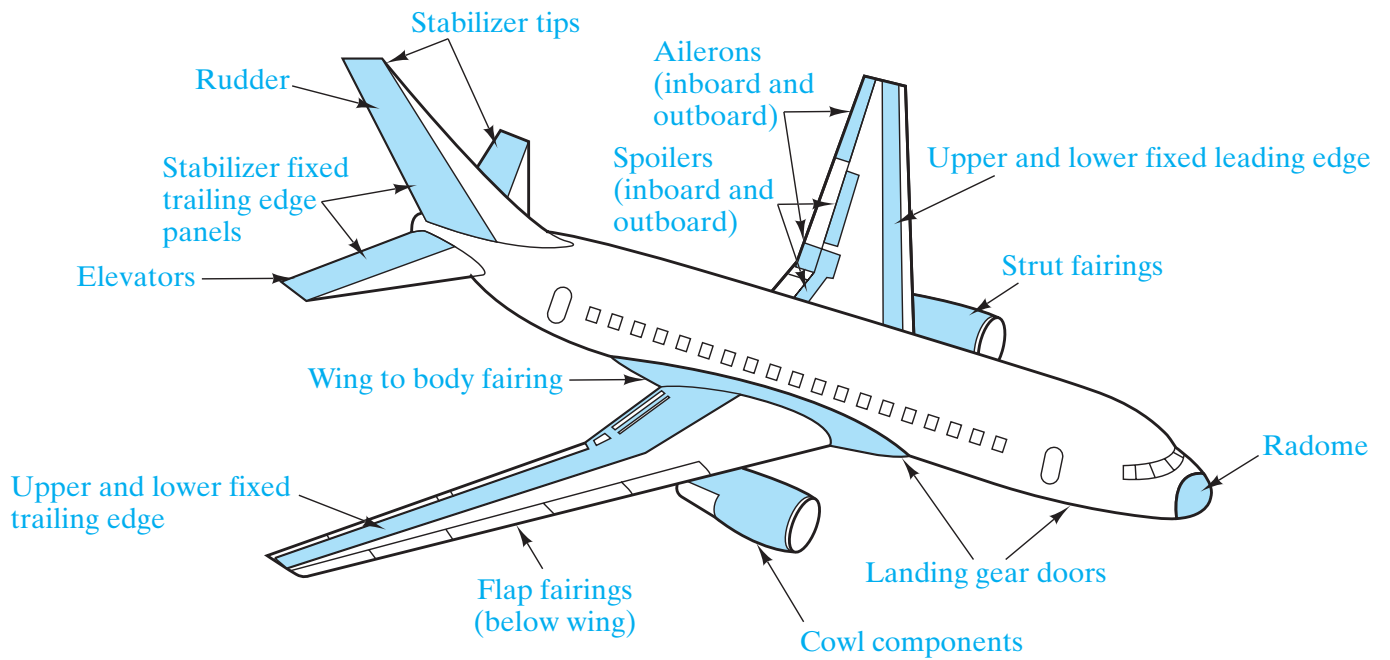


Figure 20-8 Schematic illustration of the composite structural applications for the exterior surface of a Boeing 767 aircraft. (After data from the Boeing Airplane Company.)

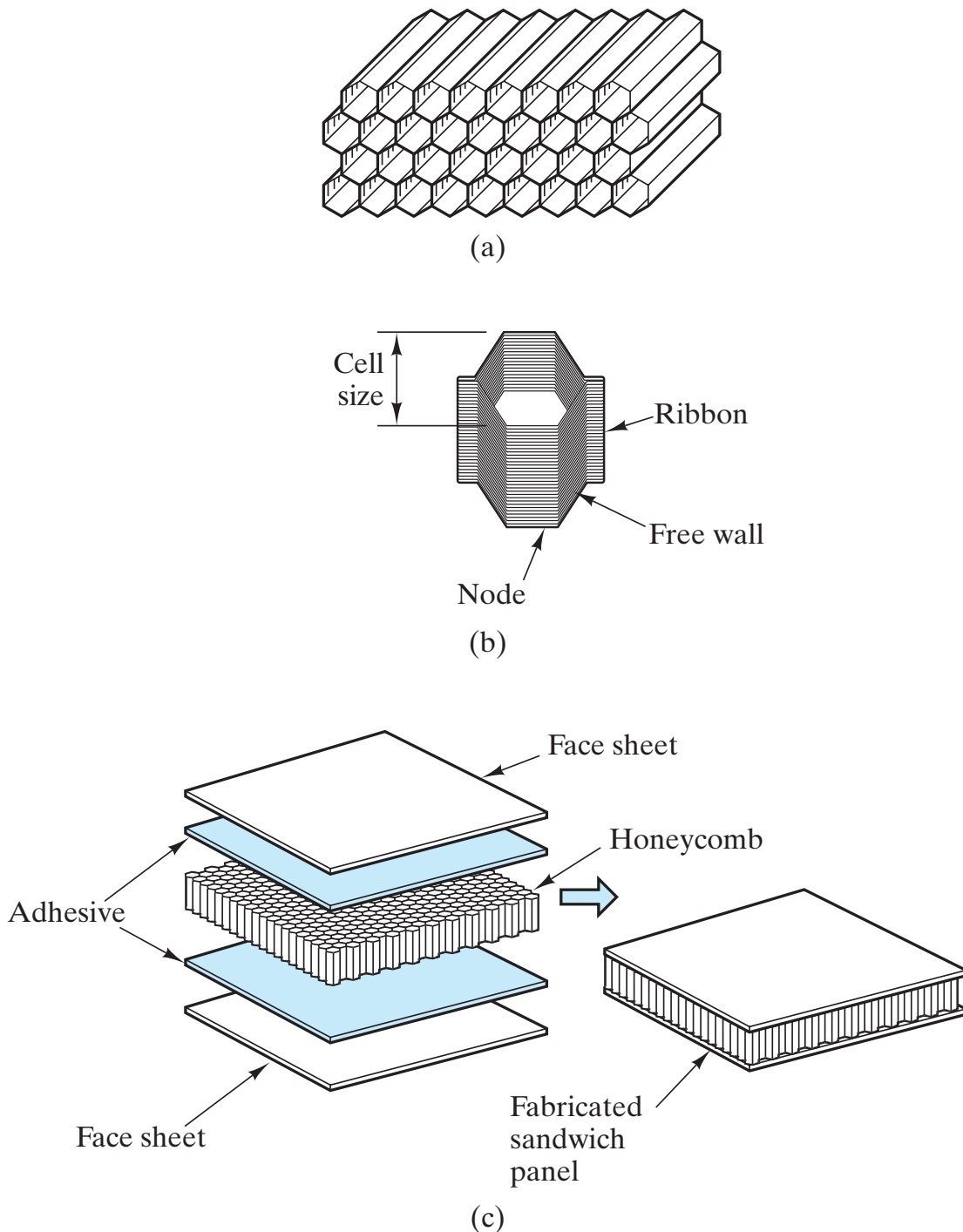
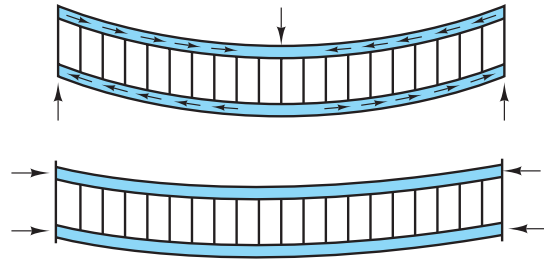
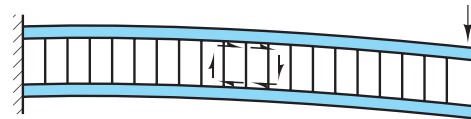


Figure 20-9 (a) Hexagonal cell honeycomb is composed of (b) individual cells composed of adhesively bonded layers which are (c) subsequently bonded to face sheets to form the overall sandwich panel. (After J. Corden, "Honeycomb Structure," in *Engineered Materials Handbook, Vol. 1, Composites*, ASM International, Metals Park, Ohio, 1987, p. 721.)

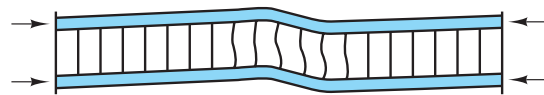
1. The facings should be thick enough to withstand the tensile, compressive, and shear stresses induced by the design load.



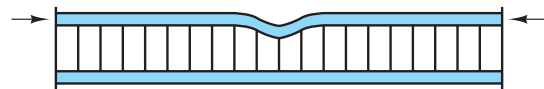
2. The core should have sufficient strength to withstand the shear stresses induced by the design loads. Adhesive must have sufficient strength to carry shear stress into core.



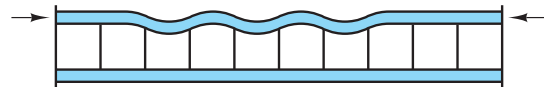
3. The core should be thick enough and have sufficient shear modulus to prevent overall buckling of the sandwich under load, and to prevent crimping.



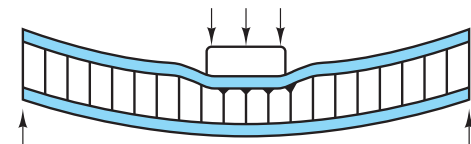
4. Compressive modulus of the core and the compressive modulus of the facings should be sufficient to prevent wrinkling of the faces under design load.



5. The core cells should be small enough to prevent intracell dimpling of the facings under design load.



6. The core should have sufficient compressive strength to resist crushing by design loads acting normal to the panel facings or by compressive stresses induced through flexure.



7. The sandwich structure should have sufficient flexural and shear rigidity to prevent excessive deflections under design load.

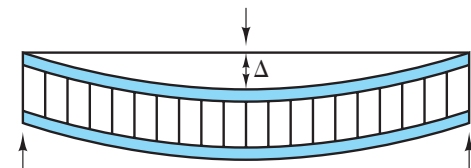


Figure 20-10 *Structural design criteria for honeycomb structural sandwich panels. (After J. Corden, "Honeycomb Structure," in Engineered Materials Handbook, Vol. 1, Composites, ASM International, Metals Park, Ohio, 1987, p. 727.)*

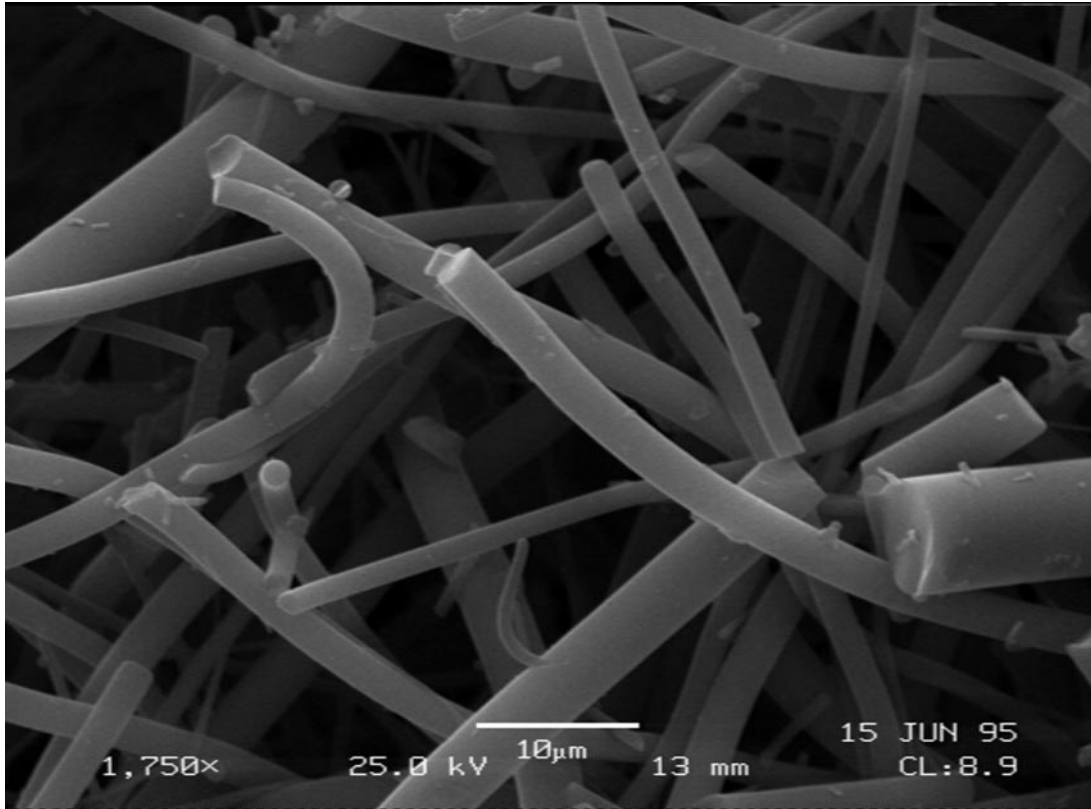


Figure 20-11 *A scanning electron micrograph of sintered silica fibers in a Space Shuttle Orbiter ceramic tile. (Courtesy of Daniel Leiser, National Aeronautics and Space Administration [NASA])*

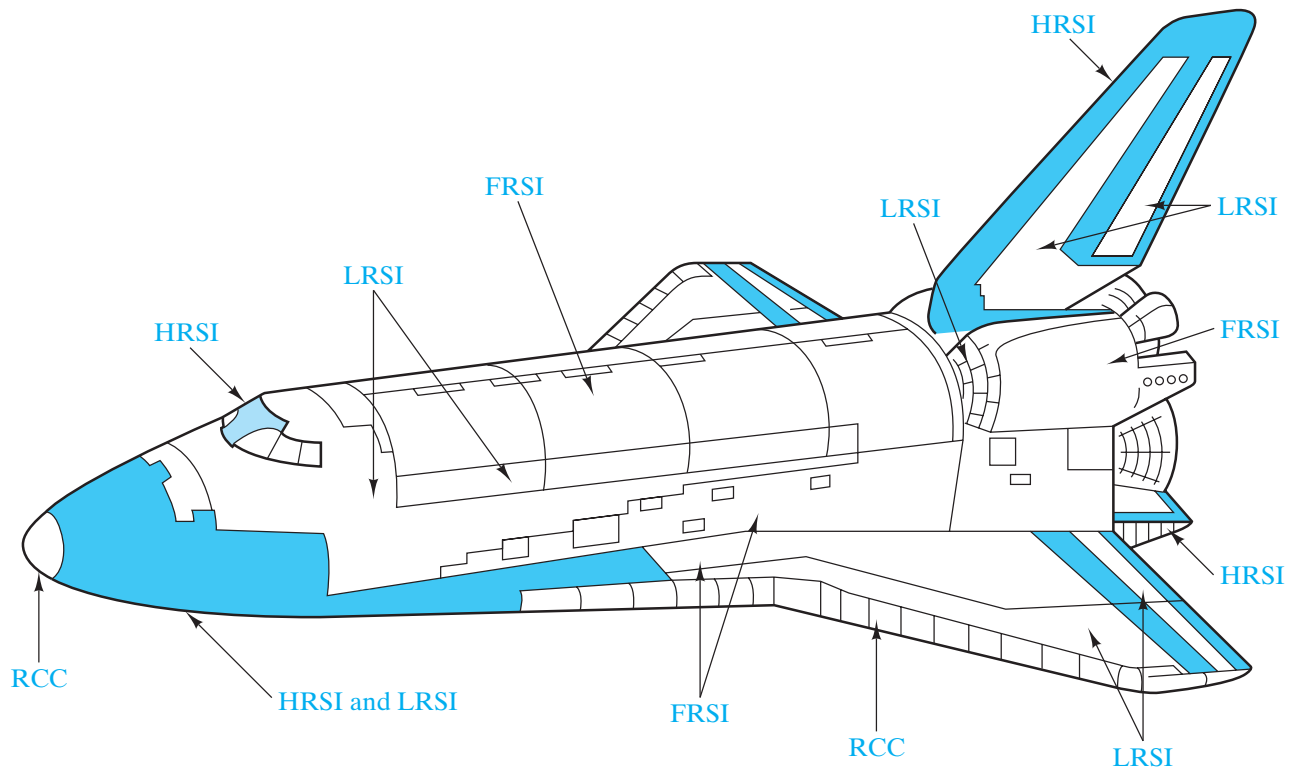


Figure 20-12 Schematic illustration of the distribution of the components of the thermal protection system for the Space Shuttle Orbiter: felt reusable surface insulation (FRSI), low-temperature reusable surface insulation (LRSI), high-temperature reusable surface insulation (HRSI), and reinforced carbon-carbon composite (RCC). (After L. J. Korb, et al., Bull. Am. Ceram. Soc. 61, 1189 [1981].)

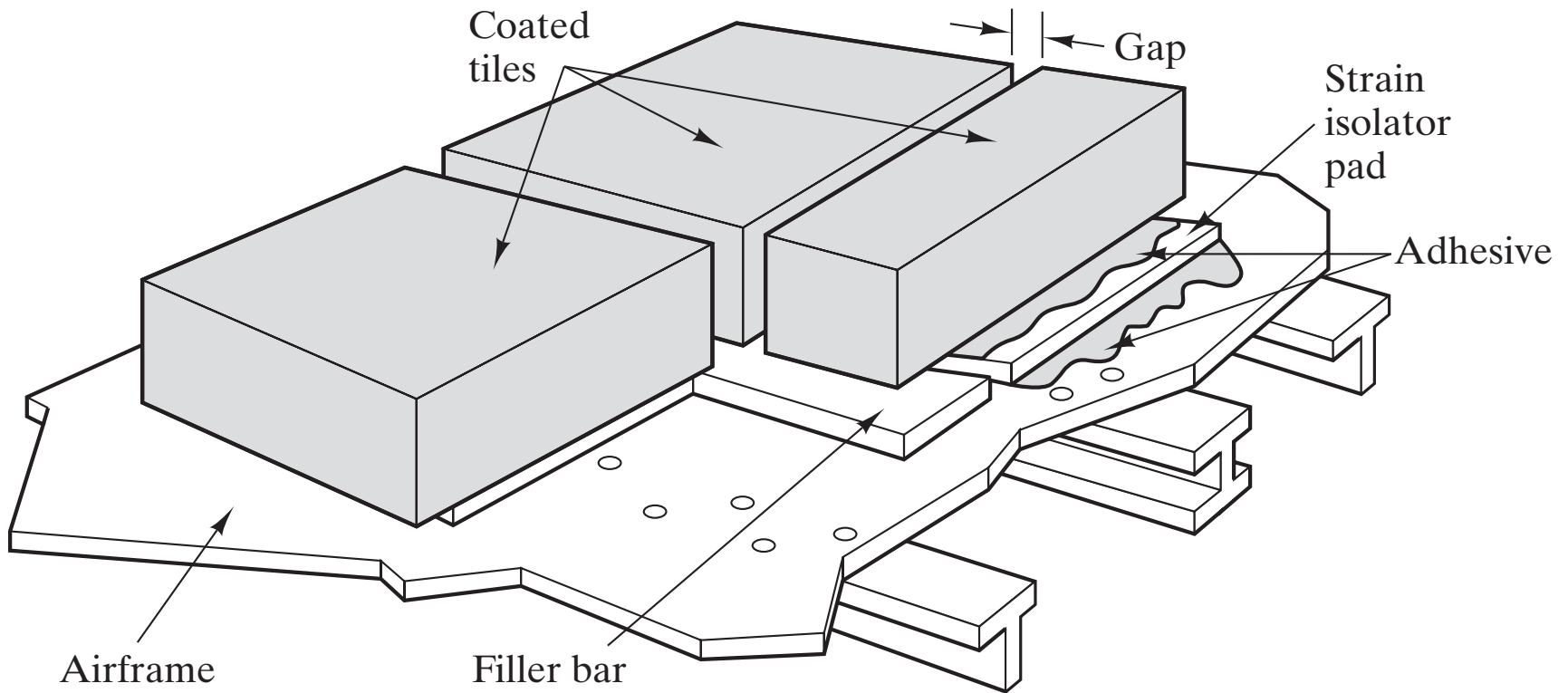


Figure 20-13 Schematic of a typical ceramic tile configuration in the thermal protection system for the Space Shuttle Orbiter. (After L. J. Korb, et al., Bull. Am. Ceram. Soc. 61, 1189 [1981].)

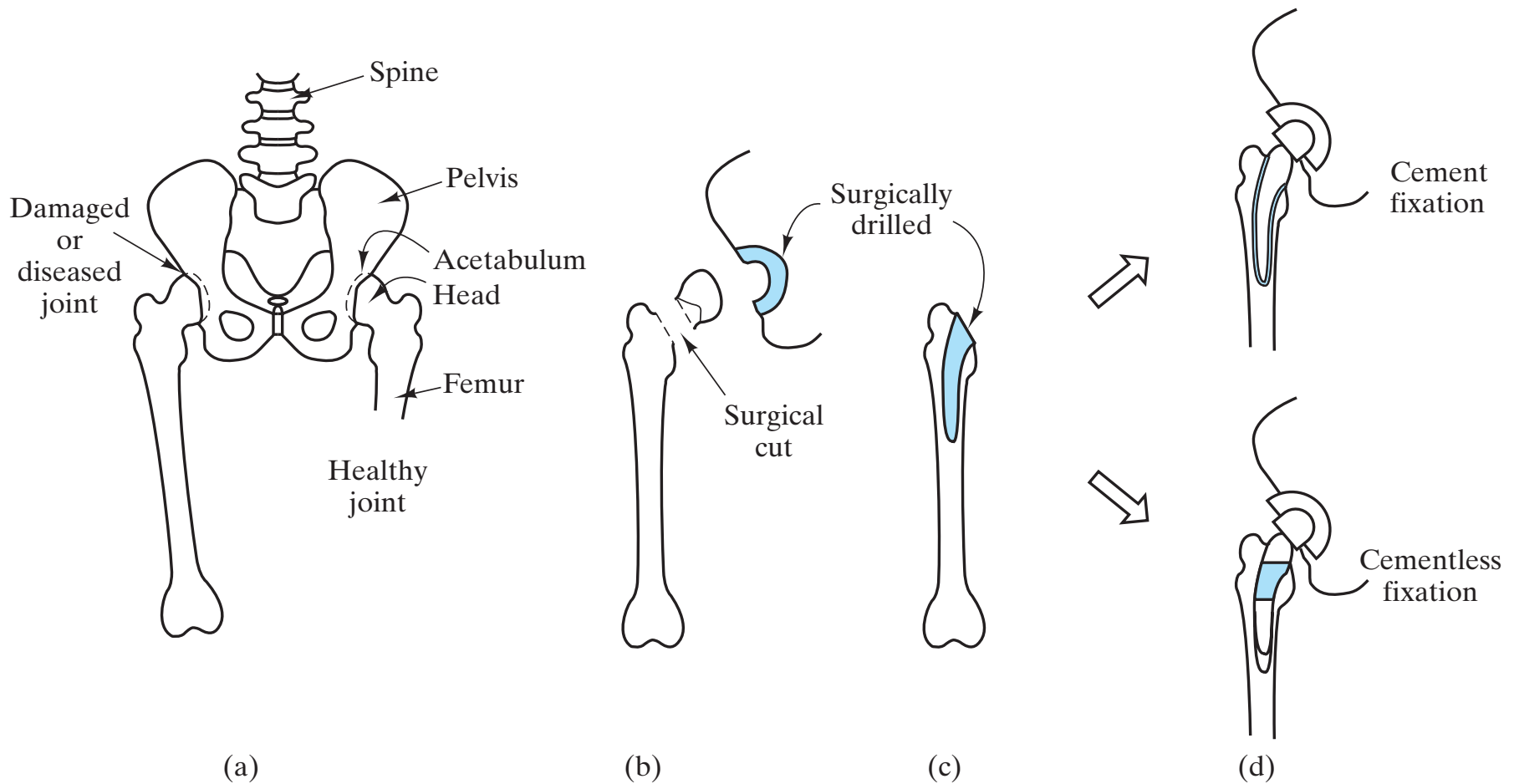


Figure 20-14 Schematic of the total hip replacement (THR) surgery. In general, the femoral implant stem is anchored to the bone by either a thin layer (a few mm thick) of polymethylmethacrylate (PMMA) cement or a cementless system involving a snug fit of the stem in the femoral shaft. In typical cementless fixation, the upper one-third of the stem is covered with a porous coating of sintered metal alloy beads. Bone growth into the porous surface provides a mechanical anchoring.



Figure 20-15 *A cobalt–chrome stem and ball, with a polyethylene cup, form a ball and socket system for an artificial hip joint. (Courtesy of DePuy, a Division of Boehringer Mannheim Corporation.)*

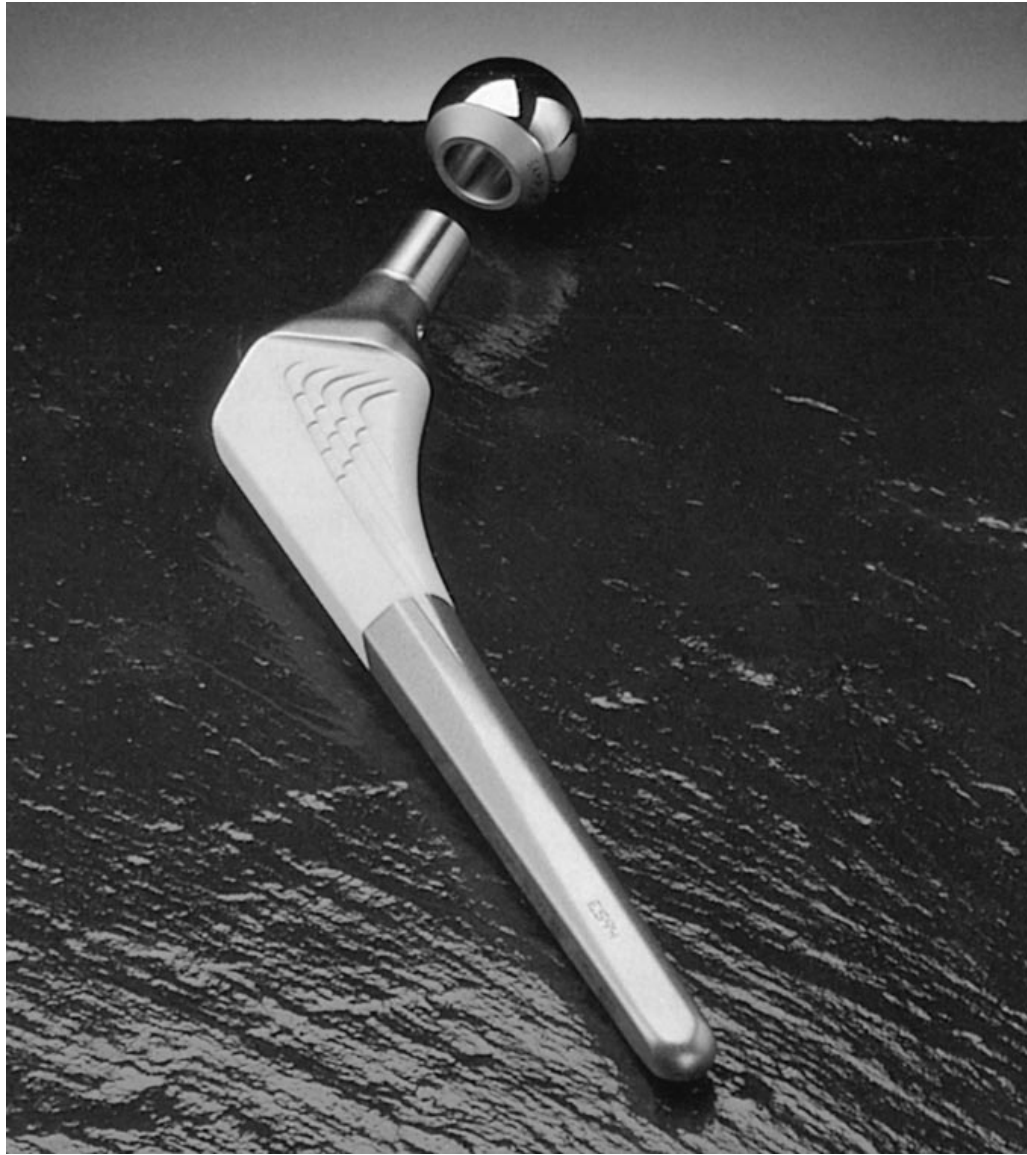
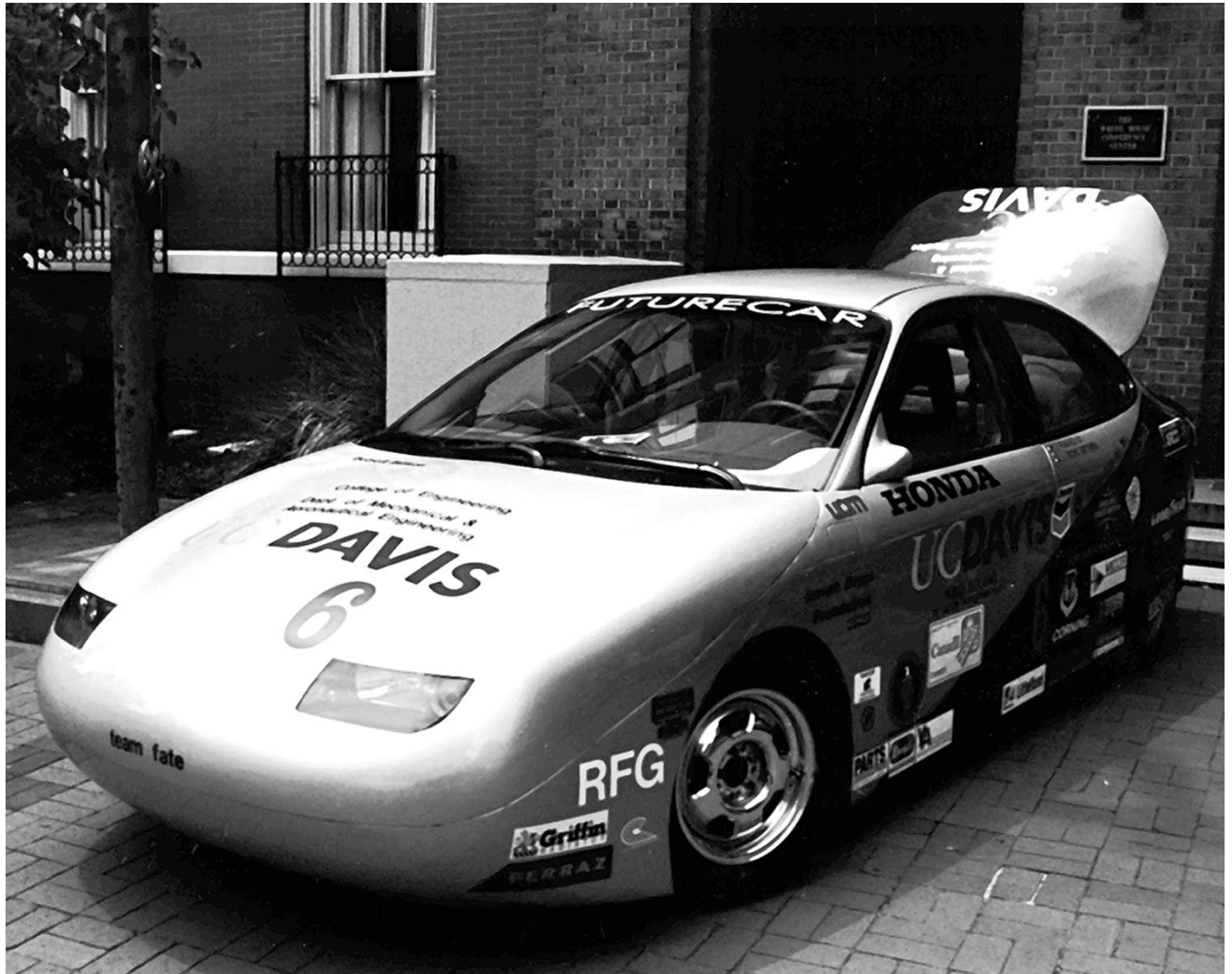


Figure 20-16 *The Omnifit® HA Hip Stem consists of hydroxyapatite coating on a hip replacement prosthesis for the purpose of improved adhesion between the prosthesis and bone. Hydroxyapatite is the predominant mineral phase in natural bone. (Courtesy of Osteonics, Allendale, New Jersey.)*



(Courtesy of the University of California, Davis)



Figure 20-17 *Transformer core winding using an amorphous ferrous alloy wire. (Courtesy of Allied-Signal, Inc.)*

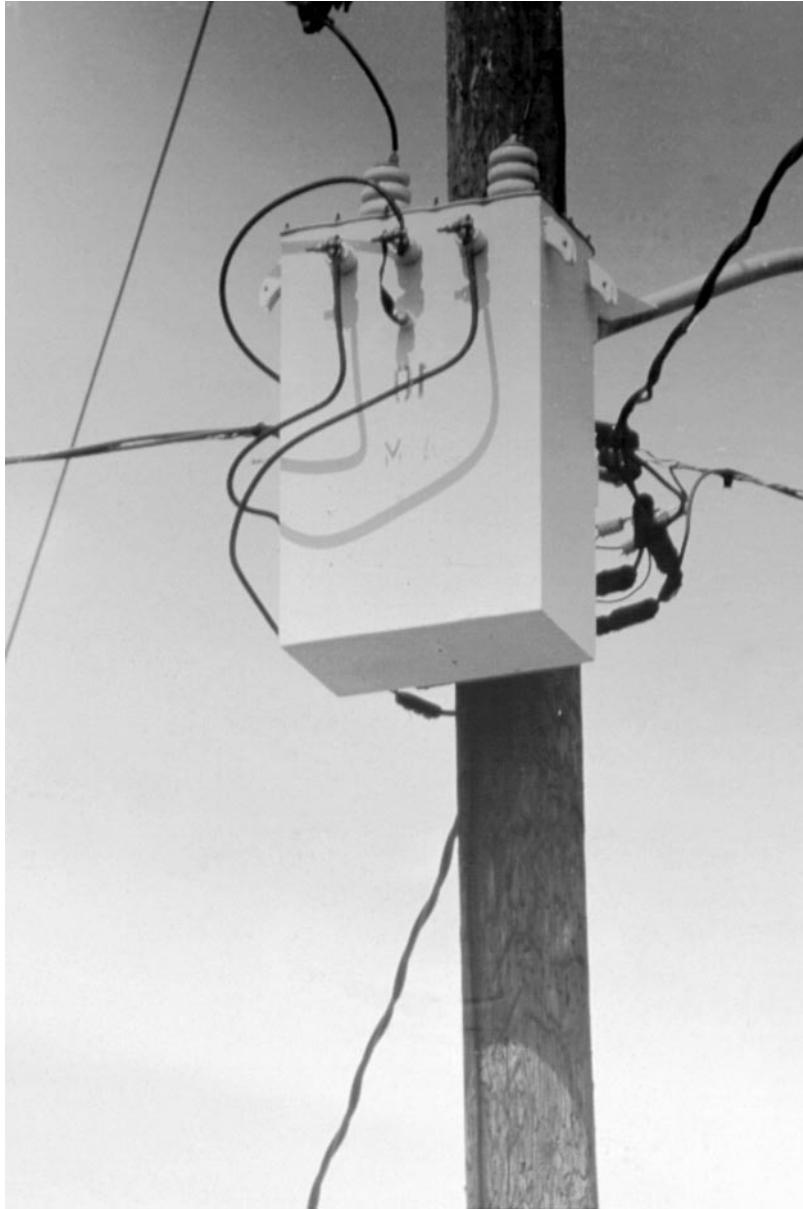


Figure 20-18 *Pole-mounted amorphous metal distribution transformer. (Courtesy of Allied Signal, Inc.)*

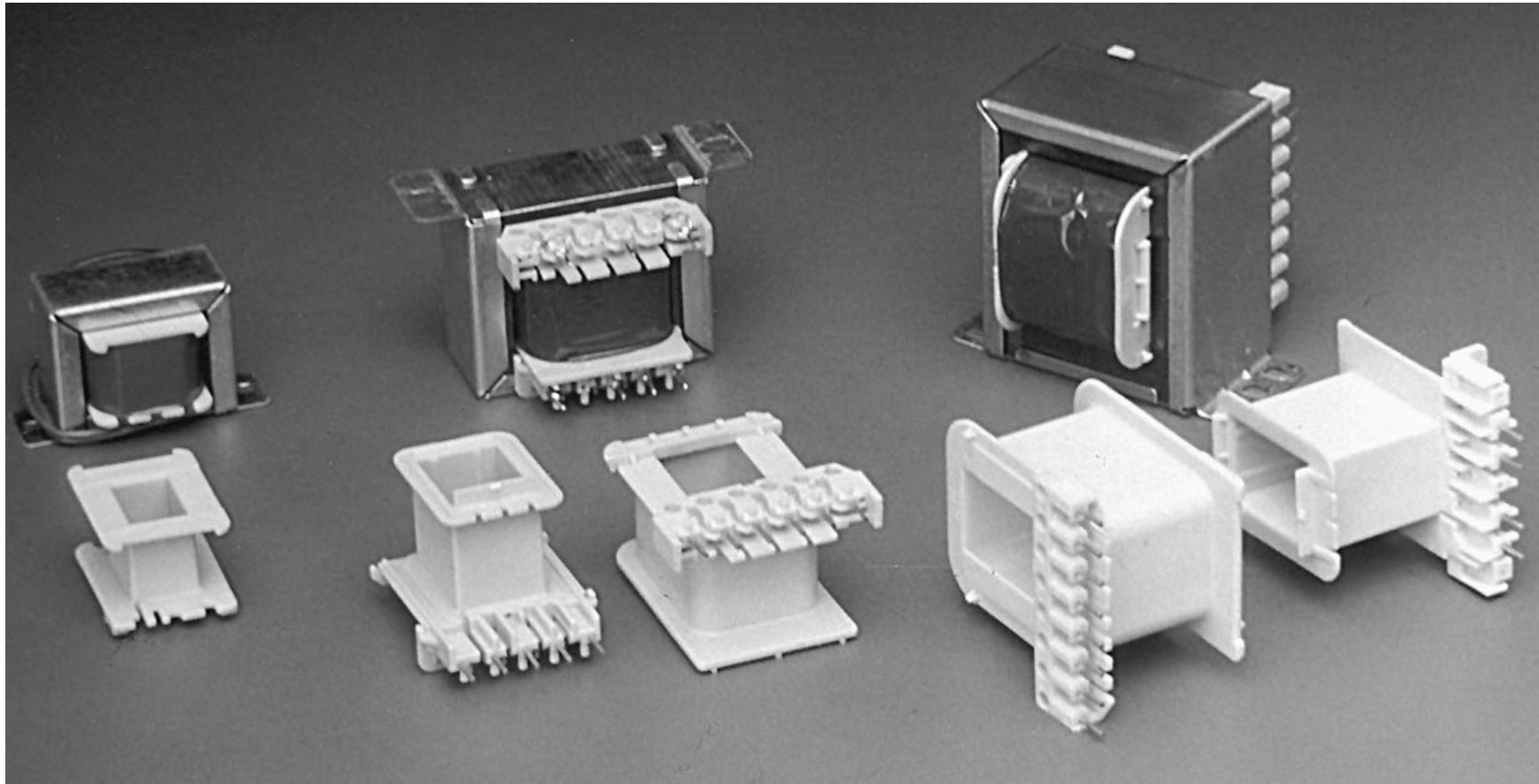


Figure 20-19 *Small transformer bobbins molded from a polyester thermoplastic are shown in the foreground. Wound, fully assembled transformers are in the background. (Courtesy of the Du Pont Company, Engineering Polymers Division.)*

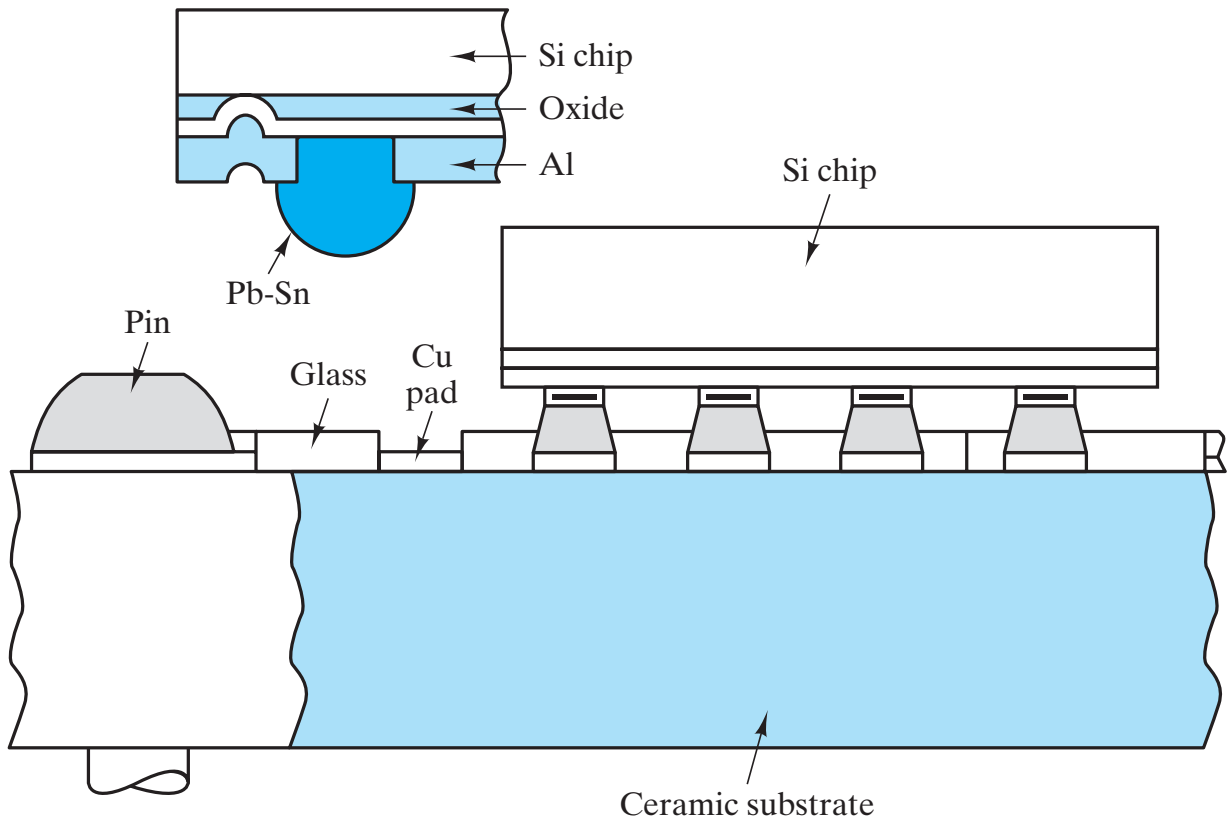


Figure 20-20 A schematic illustration of a flip-chip solder bonded to a ceramic substrate. The enlarged view shows Pb-Sn solder prior to bonding. (From J. W. Mayer and S. S. Lau, *Electronic Materials Science: For Integrated Circuits in Si and GaAs*, Macmillan Publishing Company, New York, 1990.)

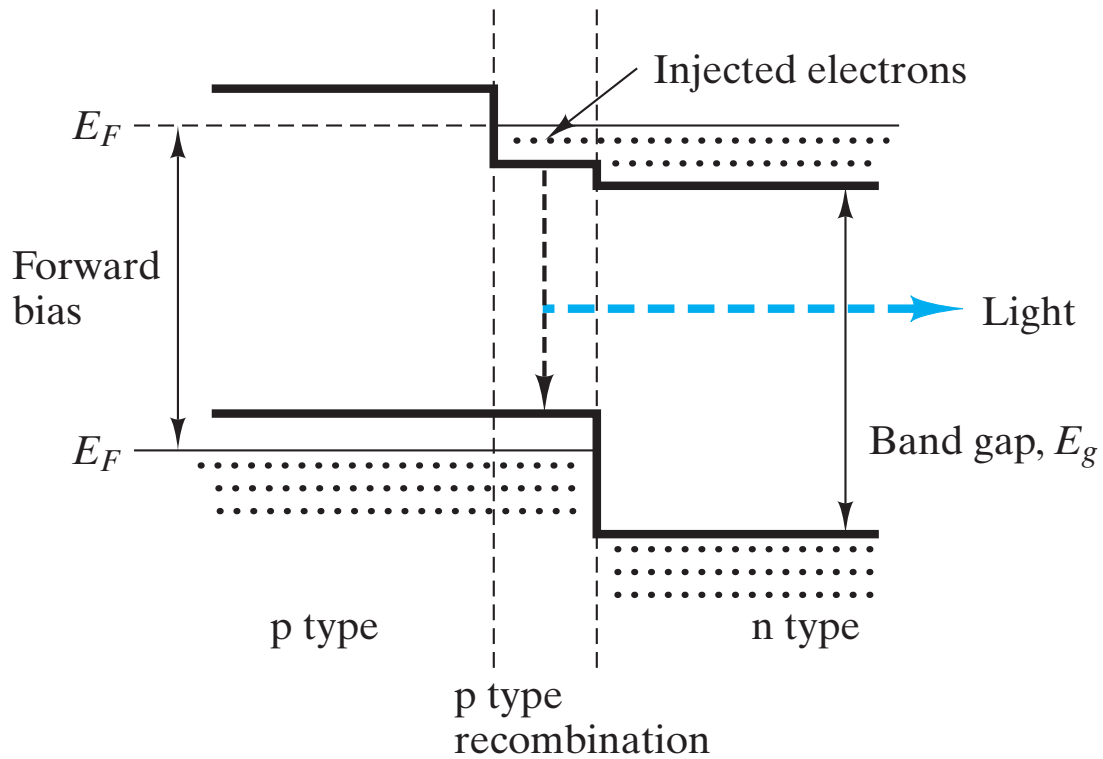


Figure 20-21 Schematic illustration of the energy band structure for a light-emitting diode (LED). (After R. C. Dorf, *Electrical Engineering Handbook*, CRC Press, Boca Raton, Florida, 1993, p. 750.)

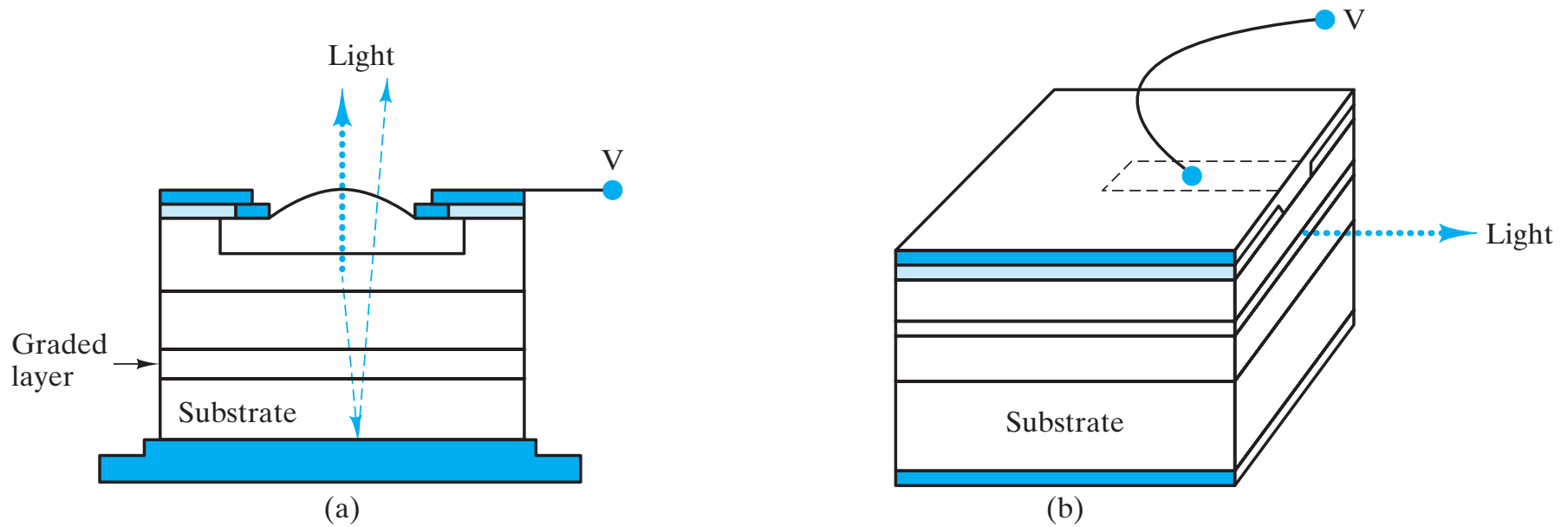


Figure 20-22 Schematic illustration of (a) surface emitting and (b) edge emitting light-emitting diodes (LEDs).
(After R. C. Dorf, *Electrical Engineering Handbook*, CRC Press, Boca Raton, Florida, 1993, p. 750.)

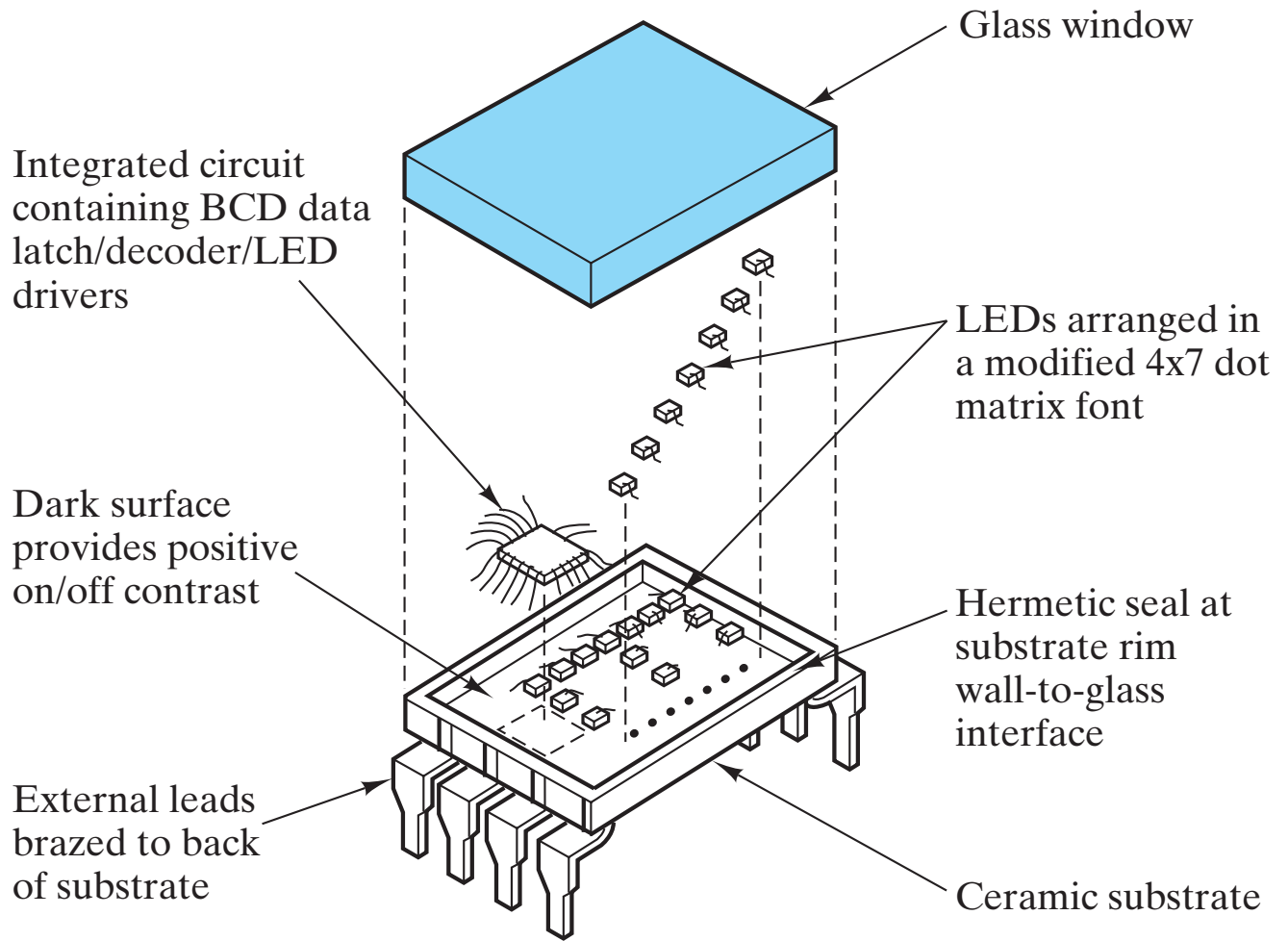


Figure 20-23 Schematic illustration of a digital display employing an array of light-emitting diodes (LED). (From S. Gage et al., *Optoelectronics/Fiber-Optics Applications Manual*, 2nd ed., Hewlett-Packard/McGraw-Hill, New York, 1981.)

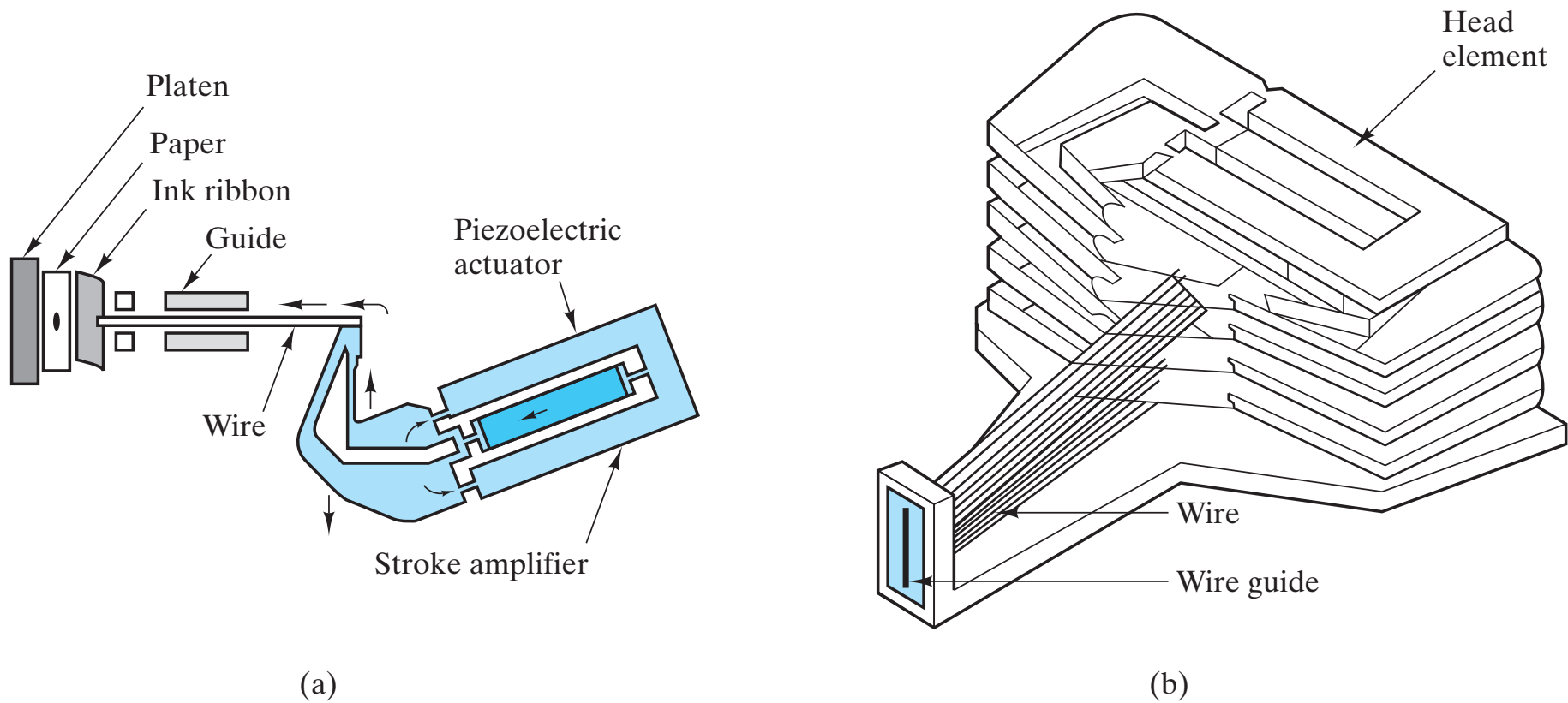


Figure 20-24 A schematic illustration of a ceramic actuator as an example of a smart material. The specific application is an impact dot-matrix printer. (a) Overall structure of the printer head. (b) Close-up of the multi-layer piezoelectric printer-head element. (From K. Uchino, MRS Bulletin, 18, 42 [1993].)

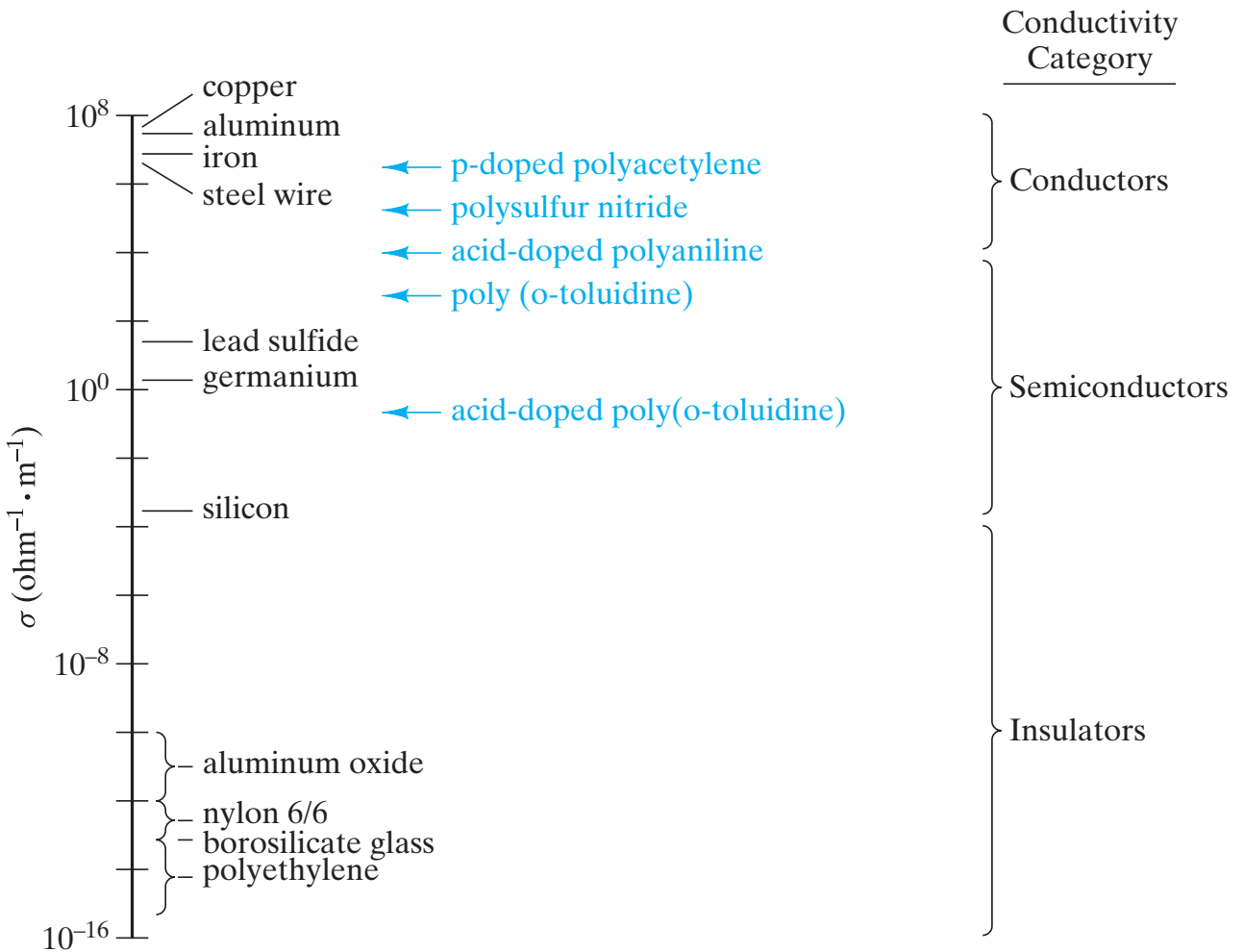


Figure 20-25 Plot of the electrical conductivity of various electronic polymers, which challenge the conventional classifications given in Figure 15-28. (After A. J. Epstein, *MRS Bulletin*, 22, 19 [1997].)

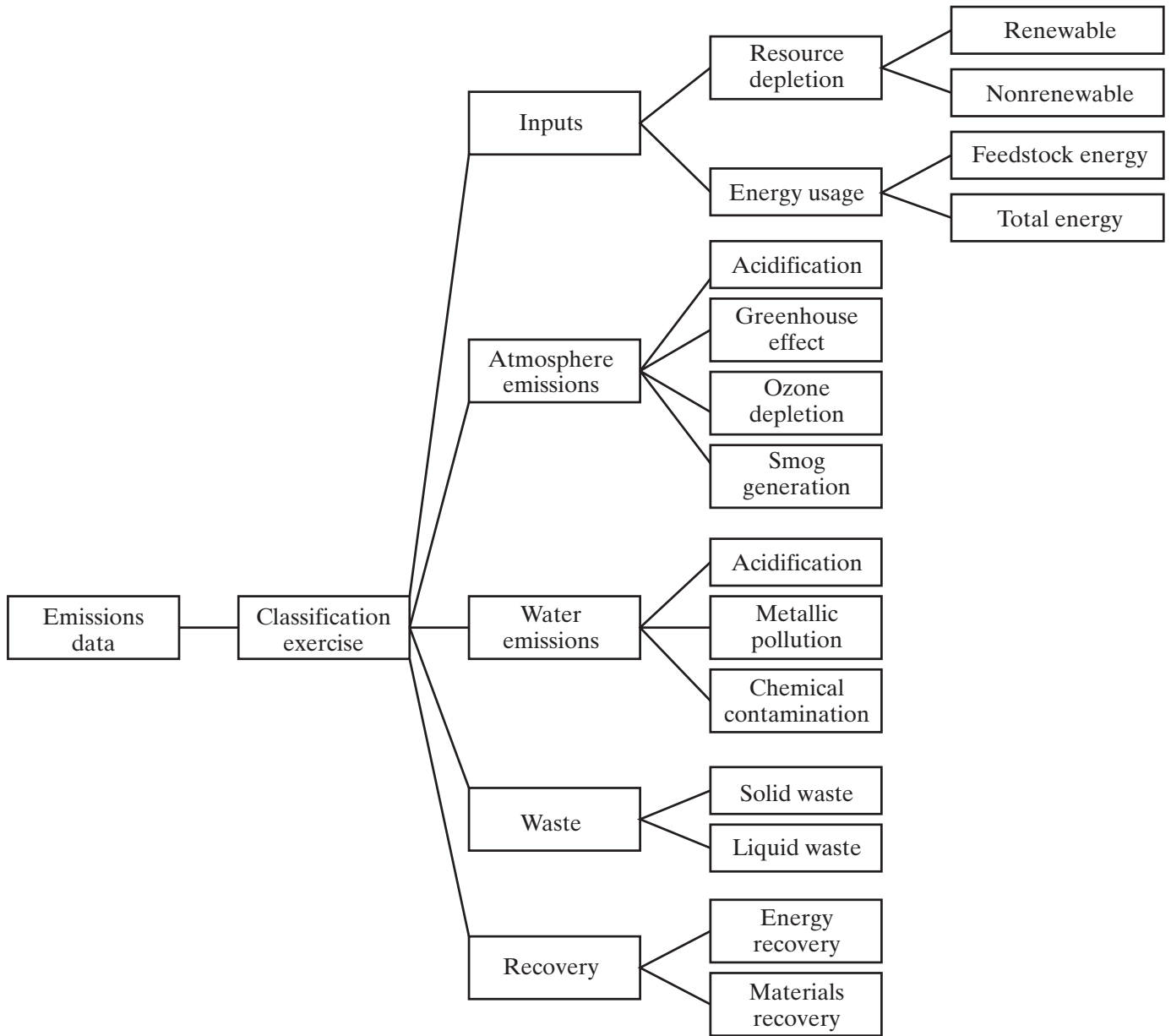


Figure 20-26 Schematic illustration of an environmental impact assessment (EIA) of emissions data. (After L. Holloway et al., *Materials and Design*, 15, 259 [1994].)

